REACTIVE PRODRUG STRATEGY FOR ADDITIVE MANUFACTURED CONTROLLED RELEASE DEVICES

Mai Di[1], Valentina Cuzzucoli Crucitti[1], Eduards Krumins[2], Anna Lion[1], Ricky Wildman[1], Vincenzo Taresco[2*] and Yinfeng He[1,3*]

[1] Faculty of Engineering, University of Nottingham, Nottingham, NG7 2RD, United Kingdom

[2] School of Chemistry, University of Nottingham, Nottingham, NG7 2RD, United Kingdom

[3] Nottingham Ningbo China Beacons of Excellence Research and Innovation Institute, University of Nottingham Ningbo China, Ningbo, China

*corresponding author: Yinfeng.he@nottingham.edu.cn, Vincenzo.taresco@nottingham.ac.uk

Abstract. Additive manufacturing technology holds significant promise in the pharmaceutical industry due to its flexibility and precision. Specifically, light-curing-based techniques like inkjet 3-D printing (IJ3DP), stereolithography (SLA), and digital light processing (DLP) offer high printing precision and are solvent-free. This enables the creation of complex drug dosage forms without concerns about solvent toxicity. Controlled-release dosage forms are increasingly favored for their improved patient compliance and reduced side effects. This study focuses on designing controlled-release dosage forms using these technologies, employing a prodrug strategy where drug molecules are bound to light-cured carriers via cleavable covalent bonds. The release rate is controlled by these bonds and the surrounding environment. Prodrugs suitable for light-cured additive manufacturing were successfully synthesised, including various drugs and cleavable covalent bonds. With the addition of photoinitiators, these prodrugs can be cured faster and have a high conversion rate under UV light irradiation. The cured drug-containing castings have different mechanical properties. These findings suggest diverse applications for drug-containing materials produced through this method.

Keywords: Additive manufacturing; controlled release; drug delivery; prodrugs, digital light processing.

1 Introduction

Additive manufacturing (also known as 3D printing) is a novel and disruptive technology that enables the rapid production of complex, customised objects through precise layer-by-layer fabrication in 3D space [1-3]. In recent years, there has been a growing interest in exploring the potential of additive manufacturing in the pharmaceutical field. The features of additive manufacturing allow this technology to facilitate personalised drug production by tailoring drug formulations, dosages, and release profiles to individual patient needs [4-6]. Several studies have attempted to fabricate drug delivery systems using additive manufacturing [7-9]. There has been a product - Spritam® (levetiracetam) approved by the US Food and Drug Administration (FDA). As an oral drug specifically for the treatment of epilepsy, the manufacturing process uses a powder bed inkjet 3D printing system in which layers of powdered drug formulation are selectively deposited and bonded together using liquid adhesives [10]. The porous structure of the tablets allows them to disintegrate and dissolve quickly for easy administration [11].

Although Spritam® is a successful immediate-release tablet, few controlled release formulations have been produced using additive manufacturing techniques. Controlled release formulations reduce the frequency of drug administration and enable continuous release of the drug within an extended time [12]. This provides more convenience to patients by improving medication compliance and reducing the likelihood of missed or delayed doses [13]. In addition, controlled release could avoid peaks in drug concentration that can lead to adverse reactions, thus improving drug safety [14].

To achieve controlled release, several studies have designed drug delivery systems with complex structures such as multilayer tablets [15-17]. These dosage forms can be produced due to the advantages of additive manufacturing techniques in printing complex structures, although their controlled release effect, which is achieved through physical means, is often limited（<12h）. He et al. proposed a prodrug-based strategy [18]. In this study, ibuprofen and hydroxyethyl acrylate (HEA) were linked by ester bonding to synthesise a reactive prodrug monomer that can undergo polymerisation. This prodrug can be inkjet 3d printed (IJ3DP) based on UV curing as a solid dosage form and achieve high drug loading (58 wt%). The prepared solid dosage form releases the drug with ester bond breaking in vivo, and dissolution experiments demonstrated that the drug can be released over a longer period (>500h), and it varies with different pH environments. In addition, drug release can also be modulated by editing the structure of the delivery system or by adding hydrophilic monomers to the ink.

Based on this idea, more active prodrug monomers containing different drugs and different breakable covalent bonds were synthesised in this study. Aspirin and mexiletine are used to synthesise reactive prodrugs containing anhydrides, amides, and carbamates. The drugs chosen for the study were common and relatively versatile, with aspirin as a non-steroidal anti-inflammatory drug (NSAID) with analgesic, antipyretic, anti-inflammatory, anti-thrombotic and potentially anticancer activities, and mexiletine being used for the treatment of cardiac arrhythmia, chronic pain, and muscle stiffness [19][20]. The types of prodrugs are determined by the chemical function-

al groups of the drugs and anhydrides, amides and carbamates are commonly used in the design of prodrugs and have different chemical stability. These prodrugs can be used not only for IJ3DP, but also for light curing based additive manufacturing techniques such as stereolithography (SLA) and digital light processing (DLP). They do not require solvent containing formulations or heating of raw materials compared to other additive manufacturing techniques, which means that thermally unstable materials can be used, and toxic solvent residues can be avoided [21][22].

In this study, the casting of the synthesised pre-drug monomers was used to verify their applicability to light curing based additive manufacturing techniques. Fourier Transform Infrared Spectroscopy (FTIR) of the material before and after curing was analysed to obtain the conversion rate. Polarised light microscopy was used to observe the presence of crystalline free drug crystals in the castings. The castings were analysed for dynamic mechanics. Finally, a prodrug was selected to determine release in different chemical environments and printed.

2 Methods and Materials

2.1 Materials

All chemicals were purchased from Sigma Aldrich or Fisher Scientific and can be used without purification. Solvents were ACS grade or better.

2.2 Synthesis of Aspirin Anhydride Prodrug

Aspirin (5 g, 27.8 mmol, 1 eq.) and Triethylamine (3.5 mL, 25.0 mmol, 0.9 eq.) were dissolved in Dichloromethane (30 mL) and placed in an ice bath. Acryloyl chloride (2.0 mL, 25.0 mmol, 0.9 eq.) was dissolved in Dichloromethane (20 mL) and slowly added to the stirring mixture. After 1h, filtration was carried out to remove the chloride salt of Triethylamine. The crude was washed with saturated sodium bicarbonate, hydrochloric acid (1M) and brine. The organic phase was then dried over MgSO4, filtered, and the solvent was removed under reduced pressure. The product was a colourless liquid with a yield of 73%. ^{1}H NMR (400 MHz, $CDCl_3$): δ 8.06 (1H, dd, *J* = 7.9, 1.7 Hz, Ar*H*), 7.69 (1H, m, Ar*H*), 7.39 (1H, m, Ar*H*), 7.20 (1H, dd, *J* = 8.2, 1.2 Hz, Ar*H*), 6.64 (1H, dd, *J* = 17.1, 1.9 Hz, C*H*=CH_2), 6.28 (1H, dd, *J* = 17.1, 10.5 Hz, CH=C*H*H), 6.15 (1H, dd, *J* = 10.5, 1.0 Hz, CH=CH*H*), 2.37 (3H, s, CH_3C=0)ppm.

2.3 Synthesis of Mexiletine Amide Prodrug

Mexiletine hydrochloride (10 g, 46 mmol, 1 eq.) and Triethylamine (12 mL, 87 mmol, 1.9 eq.) were dissolved in a Dichloromethane (80 ml) and placed in ice bath. Acryloyl chloride (3.6 mL, 41 mol, 0.9 eq.) was dissolved in Dichloromethane (20 mL) and slowly added to the stirring mixture. Left stirring at 0°C for 1h and left overnight at room temperature. Filtration was carried out to remove the chloride salt of Triethylamine. The crude was washed once with hydrochloric acid (1M) and twice with brine.

The organic phase was then dried over MgSO4, filtered, and the solvent was removed under reduced pressure. The product was a white solid with a yield of 68%.^{1}H NMR (400 MHz, $CDCl_3$): δ 7.01 (3H, m, Ar*H*), 6.34 (1H, dd, *J* = 17.0, 1.5 Hz, C*H*=CH_2), 6.16 (1H, dd, *J* = 17.0, 10.3 Hz, CH=*CH*H), 6.10 (1H, s, N*H*), 5.70 (1H, dd, *J* = 10.2, 1.5 Hz, CH=CH*H*), 4.46 (1H, m, C*H*CH_3), 3.83 (2H, m, CHCH_2) 2.28 (6H, s, 2×CH_3), 1.48 (3H, d, *J* = 6.8 Hz, C*H*3CH)ppm.

2.4 Synthesis of Mexiletine carbamate Prodrug

N, N'-Disuccinimidyl carbonate (4.90 g, 19.1 mmol, 1.1 eq.) was dissolved in 40 mL DCM and placed in an ice bath. 2-Hydroxyethyl acrylate (2 mL, 17.4 mmol, 1 eq.) and pyridine (1.4 mL, 17.4 mmol, 1 eq.) were dissolved in Dichloromethane (20 mL) and slowly added to the solution. The reaction was left stirring for 1h in the ice bath. The crude was washed with hydrochloric acid (1M), sodium hydroxide (1M) and brine. The organic phase was then dried over MgSO4, filtered, and the solvent was removed under reduced pressure. The obtained 2-((((2,5-dioxo-2,5-dihydro-1H-pyrrol-1-yl)oxy)carbonyl)oxy)ethyl acrylate was used for the next reaction. ^{1}H NMR (400 MHz, $CDCl_3$): δ 6.49 (1H, dd, *J* = 17.3, 1.3 Hz, C*H*=CH_2), 6.18 (1H, dd, *J* = 17.3, 10.5 Hz, CH=*CH*H), 5.92 (1H, dd, *J* = 10.5, 1.3 Hz, CH=CH*H*), 4.52 (4H, m, OCH_2CH_2O), 2.86 (4H, s, O=CCH_2C$H_{2C=}$O).
2-((((2,5-dioxopyrrolidin-1-yl)oxy)carbonyl)oxy)ethyl acrylate (1 g, 3.9 mmol, 1 eq.) was dissolved in 5ml DCM. Mexiletine hydrochloride (0.93 g, 4.3 mmol, 1.1 eq.) and pyridine (0.35 mL, 4.3 mmol 1.1 eq.) were dissolved in Dichloromethane (10 mL) and slowly added to the string solution. The reaction was left stirring overnight. The crude was washed with hydrochloric acid (1M), sodium hydroxide (1M) and brine. The organic phase was then dried over MgSO4, filtered, and the solvent was removed under reduced pressure. The product was a white solid with a yield of 52%. ^{1}H NMR (400 MHz, $CDCl_3$): δ 6.99 (3H, m, Ar*H*), 6.46 (1H, d, *J* = 17.4 Hz, CH=CH*H*), 6.17 (1H, dd, *J* = 17.3, 10.4 Hz, C*H*=CH_2), 5.88 (1H, m, CH=CH*H*), 5.15 (1H, s, N*H*), 4.37 (4H, d, *J* = 7.5 Hz, OCH_2CH_2O), 4.09 (1H, m, C*H*CH_3), 3.76 (2H, m, CHCH_2), 2.28 (6H, s, 2×CH_3), 1.43 (3H, d, *J* = 6.8 Hz, CH_3CH).

2.5 Nuclear Magnetic Resonance (NMR)

The samples were analysed by 1H NMR, using a Bruker 400 Ultrashield (400 MHz NMR), and all the samples were dissolved in deuterated chloroform. Spectra were processed using MestReNova version 9.0.1 (Mestrelab Research, Santiago de Compostela, Spain).

2.6 Fourier Transform Infrared Spectroscopy (FTIR)

A Frontier FT IR-ATR (Perkin Elmer) was used to analyse the ink formulation and printed samples. All the specimens were scanned between 600 cm^{-1} and 4000cm^{-1} with a step of 0.5 cm^{-1}.

2.7 Electrospray Ionisation Time-of-Flight Mass Spectroscopy (ESI-TOF MS)

A Focus Micro TOF spectrometer from Bruker Daltonics (Billerica, MA, USA) was used to conduct ESI-TOF MS measurements. A total of 1 mg of the sample was dissolved in HPLC grade THF at a final concentration of 10 µL/mL. The measured data were interpreted using Data Analysis 4.2 software from Bruker Daltonics.

2.8 Ink Preparation and Casting

N-acryloyl morpholine (1 g) was added to mexiletine prodrug (1 g) and carbamate prodrug (1 g) respectively and heated to 50° on a hot plate to obtain liquid formulations. Then, the photoinitiator 2,2-Dimethoxy-2-phenylacetophenone (0.02 g) was added to the two formulations obtained above and aspirin anhydride prodrug (2 g). The inks were stirred at room temperature and protected from light until the photoinitiator was completely dissolved, then dropped into the moulds and cured under a UV LED lamp (peak irradiance = 1.5 W/cm², wavelength = 365 nm) for 30 seconds, resulting in samples with lengths, widths, and heights of approximately 30 mm, 10 mm, and 1 mm, respectively.

2.9 Microscopic Analysis

The Nikon LV150NL Upright Materials Microscope with the addition of a polariser analyser was used to observe whether there are crystals composed of free drug molecules in casting samples. Under cross-polarised light, the casting samples are imaged using a ×10/0.4 NA objective lens (UPLSAPO 10X, Olympus), captured with DS-Fi2 high-definition colour camera head, which has 640 × 480 pixels.

2.10 Dynamic Mechanical Analysis

To test the mechanical properties of the cured prodrug, a Triton Technology Dynamic Mechanical Analyser was used to perform Dynamic Mechanical Analysis (DMA) on the casting samples. Samples were analysed in tension mode, with a frequency of 1 Hz, a dynamic force of 1 N. Tests were performed in triplicate.

2.11 Dissolution Test

The USP Apparatus 1 (basket) was used to test the release of casting samples using a Copley DIS 8000 dissolution tester. Samples made by aspirin anhydride prodrug were placed in the basket and the rotational speed was 50 rpm. The dissolution medium was 500 ml of buffer solution (pH 2 and pH 7.4) maintained at 37 ± 0.5°C. At appropriate time intervals, a sample of the solution (1 ml) was removed from the dissolution apparatus and the volume of the sample was replaced with a fresh dissolution medium. After filtration through a polytetrafluoroethylene (PTFE) filter membrane (0.45 µm pore size), 300 µl was pipetted into a quartz 96-well plate. Subsequently, the

samples were analysed in a directional manner at 265 nm using a Tecan Spark multi-mode microplate reader. Three parallel experiments were recorded.

To determine the association between the released aspirin concentration and the UV absorption, a calibration curve was plotted. Aspirin was dissolved in a phosphate buffer solution at pH 2 and pH 7.4 to make solutions at concentrations of 0.2, 0.15, 0.1, 0.075, 0.05, 0.0375, 0.025, 0.0125 and 0.00625 mg/mL. The UV absorption was measured using a microplate spectrophotometer.

2.12 DLP 3D Printing

The Lumen X (Cellink) DLP 3D printer was used to print the formulation of aspirin anhydride prodrug. In addition to the prodrug and photoinitiator, 0.1% wt of the photo masking agent curcumin was added to the ink to avoid overexposure. The printer was equipped with a diode with an emission wavelength of 405 nm and the thickness of the printed layer was 100 μm. The exposure time was set to 10 s for both the body and the base.

3 Results and Discussions

3.1 Synthesis of Aspirin Anhydride Prodrug

Scheme 1 shows the reaction for the synthesis of the aspirin anhydride prodrug. Initially, higher amounts of triethylamine and acryloyl chloride (1.2 molar equivalents to aspirin) were used to increase the conversion of aspirin to the anhydride prodrug. However, 4 hours after the start of the reaction, the colour of the mixture gradually changed to dark brown. After washing, the sample remained orange in colour (Fig. 1). According to the literature, this colour may arise from the formation of a biotoxic complex between acryloyl chloride and triethylamine [23]. Subsequently, the amounts of triethylamine and acryloyl chloride were reduced （0.9 eq.） and the reaction time was shortened to 1 hour. A colourless oily product was obtained in a 73% yield.

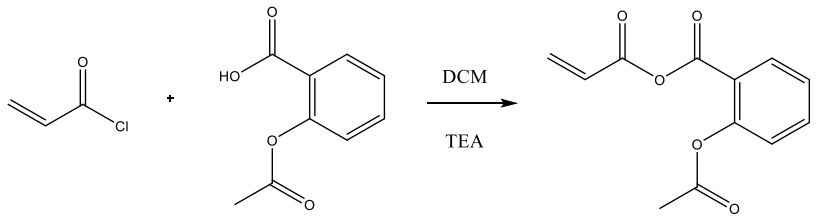

Scheme 1. Synthesis of aspirin anhydride prodrug.

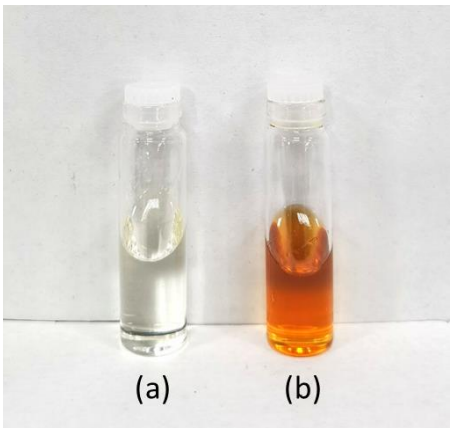

Fig. 1. Pictures of a) pure aspirin anhydride prodrug; b) product with impurities after purification.

Fourier-transform infrared spectroscopy (FTIR) was used for the confirmation of the successful conversion of aspirin to the anhydride prodrug (Fig. 2). The spectrum of aspirin shows a broad band in the range of 2200-3300 cm^{-1} (O-H stretching of the hydroxyls within the carboxylic acid groups) and two distinct carbonyl peaks at 1750 cm^{-1} and 1680 cm^{-1} (C=O stretching of carboxylic acid and ester). In the spectrum of the product, it is hard to observe the broad peaks representing O-H stretching. Besides the carbonyl peaks at 1766 cm^{-1} (stretching vibration of ester C=O), there are two additional carbonyl peaks at 1774 cm^{-1} (stronger) and 1725 cm^{-1} (weaker). These two peaks are characteristic of unsaturated anhydrides [24].

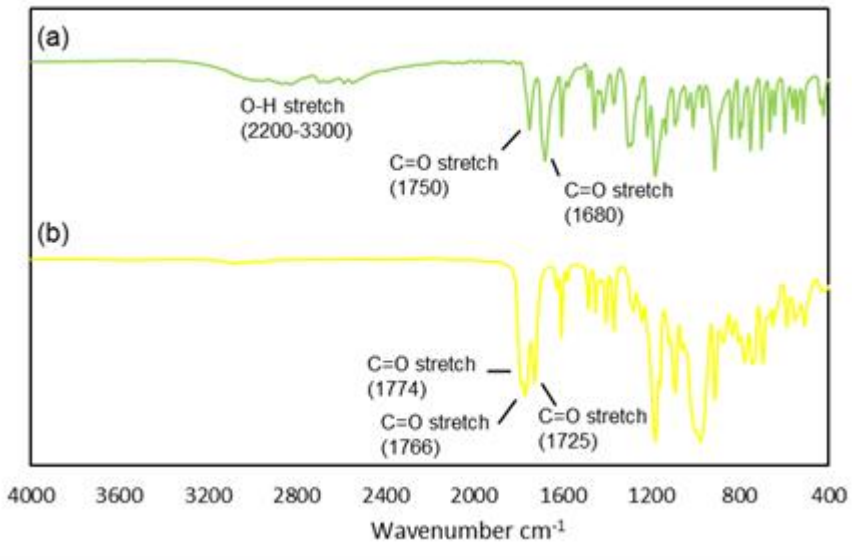

Fig. 2. FTIR spectrum of a) aspirin; b) aspirin anhydride prodrug.

According to the ^{1}H-NMR spectrum (Fig. 3), the integration of the peak areas shows a 1:1 ratio of aspirin to acryloyl in the product, which is consistent with the theoretical peak area ratio of the prodrug molecule. Furthermore, ESI-MS analysis produced one characteristic fragment ion at m/z=257 which corresponds to $[C_{12}H_{10}O_5 + Na]^+$. This also proves the successful synthesis of the aspirin prodrug.

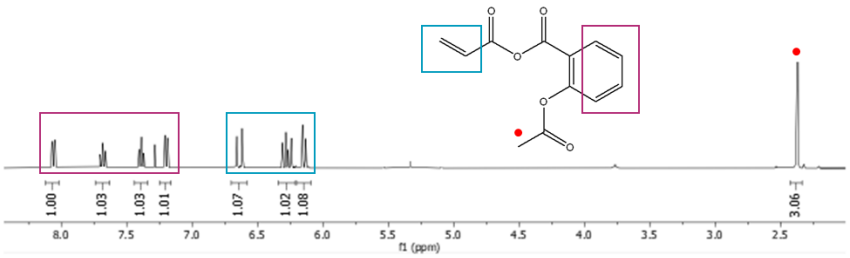

Fig. 3. ^{1}H-NMR spectrum of aspirin anhydride prodrug.

3.2 Synthesis of Mexiletine Amide Prodrug

Scheme 2 shows the reaction for the synthesis of mexiletine amide prodrug. FTIR was used to detect whether mexiletine hydrochloride was formed amide prodrug with acryloyl chloride (Fig. 4). The spectrum of mexiletine hydrochloride showed a broad peak between 2800-3000 cm^{-1} (N-H stretch), which transformed into a narrow peak at 3268 cm^{-1} in the spectrum of the product. In addition, the peaks (N-H bend) at 1612 cm^{-1} and 1657 cm^{-1} in the spectrum of mexiletine hydrochloride, respectively, converted into a more intense peak at 1653 cm^{-1} in the spectrum of the product. This is due to the conjugation occurring in the amide resulting in a higher wave number and more intense of the bend. The C=0 stretch signal located at 1725 cm^{-1} also proves the formation of amide.

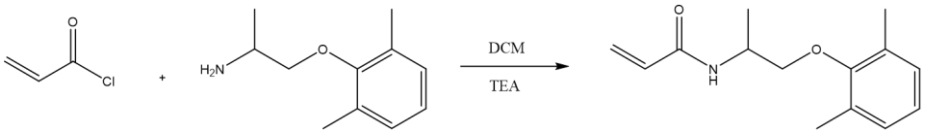

Scheme 2. Synthesis of mexiletine amide prodrug.

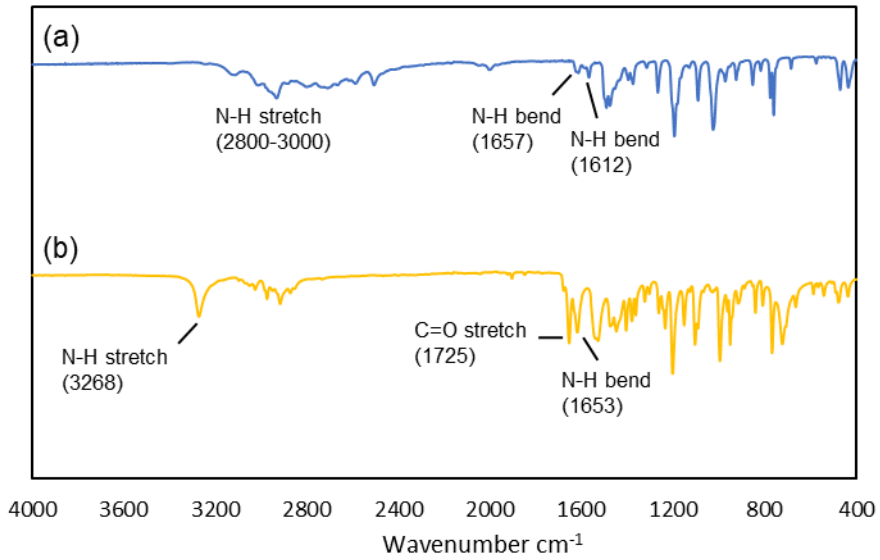

Fig. 4. FTIR spectrum of a) mexiletine hydrochloride; b) mexiletine amide prodrug.

Based on the ^{1}H-NMR spectral analysis of the product, it has been observed that only one amide hydrogen (6.10 ppm) is present (as shown in Fig. 5). By calculating the peak area integral, it has been determined that the ratio of mexiletine and acryloyl is 1:1. This indicates that equal amounts of mexiletine and acryloyl are combined through amide bond. Additionally, on analysing the ESI-MS results, a characteristic peak corresponding to [C14H20NO2 + H] $^{+}$ has been identified at m/z = 234. This suggests the presence of mexiletine amide prodrug.

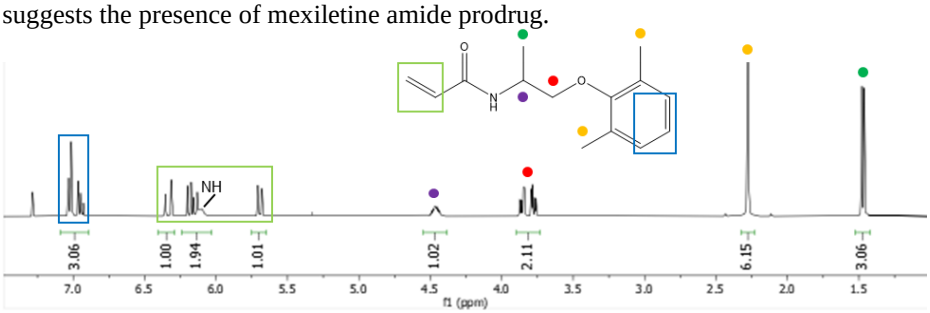

Fig. 5. ^{1}H-NMR spectrum of mexiletine amide prodrug.

3.3 Synthesis of Mexiletine Carbamate Prodrug

Scheme 3 shows the synthetic reaction of the mexiletine carbamate prodrug. Pyridine was used in this two-step reaction instead of the more basic triethylamine to avoid rearrangement reactions. The formation of the carbamate prodrug was determined by

comparing the FTIR spectra of the reactants and products (Fig. 6). The hydroxyl O-H stretch (3000-3600 cm^{-1}) in the spectrum of Hydroxyethyl acrylate could not be observed in the product spectra. The ammonium salt N-H stretch (2800-3000 cm^{-1}) in the spectrum of mexiletine hydrochloride was converted into the final product spectrum representing the amide/carbamate N-H stretch (3311 cm^{-1}) in the final product spectrum. The C=0 stretch signals located at 1842 cm^{-1} and 1760 cm^{-1} in the spectrum of coupling agent N,N'-Disuccinimidyl carbonate could not be observed in the product spectrum, indicating substitution of the two succinimides.

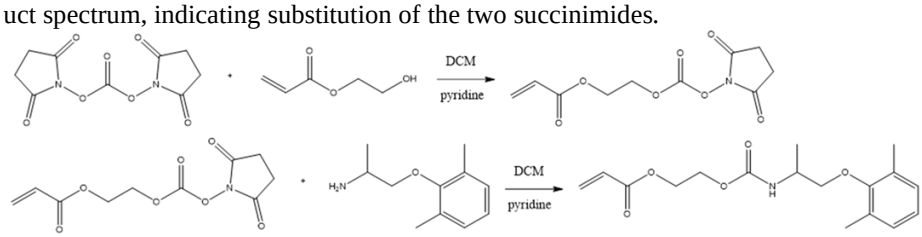

Scheme 3. Synthesis of mexiletine carbamate prodrug.

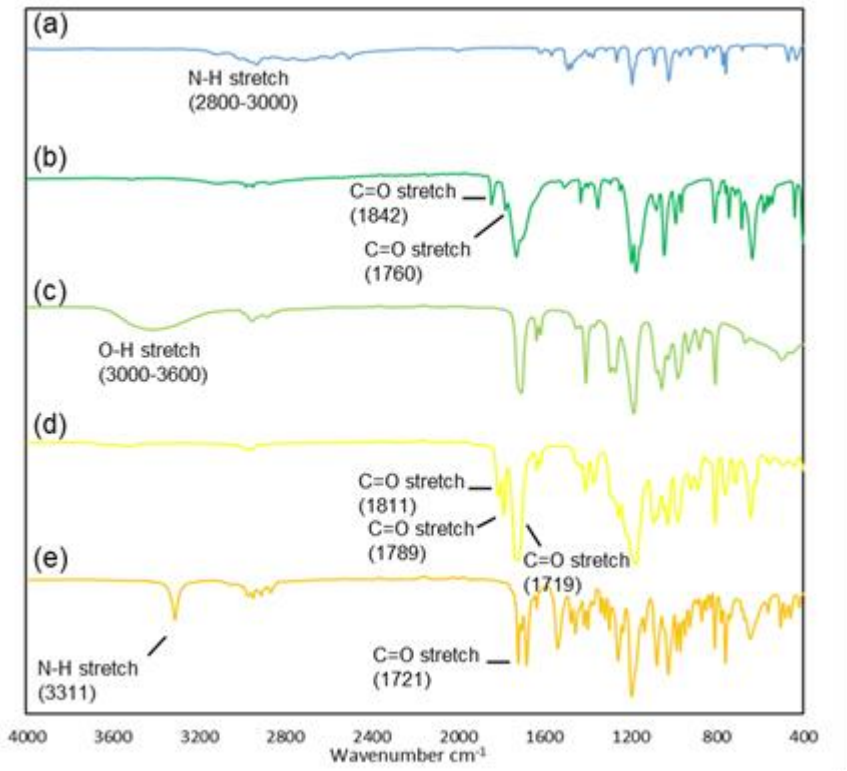

Fig. 6. FTIR spectrum of a) mexiletine hydrochloride; b) N,N'-Disuccinimidyl carbonate; c) hydroxyethyl acrylate; d) 2-((((2,5-dioxopyrrolidin-1-yl)oxy)carbonyl)oxy)ethyl acrylate; e) mexiletine carbamate prodrug.

According to the ^{1}H-NMR results (Fig. 7), there was no peak observed at 2.86 ppm with an integration of 4 in the final product spectrum. This indicates that the succinimide of 2-((((2,5-dioxopyrrolidin-1-yl)oxy)carbonyl)oxy)ethyl acrylate is completely substituted by mexiletine in the second reaction step. The peak area integral of the final product spectrum is consistent with the theoretical value of mexiletine carbamate prodrug. The products were characterised by ESI-MS and a peak at m/z = 344 was observed, which corresponds to $[C17H23NO5 + Na]^{+}$.

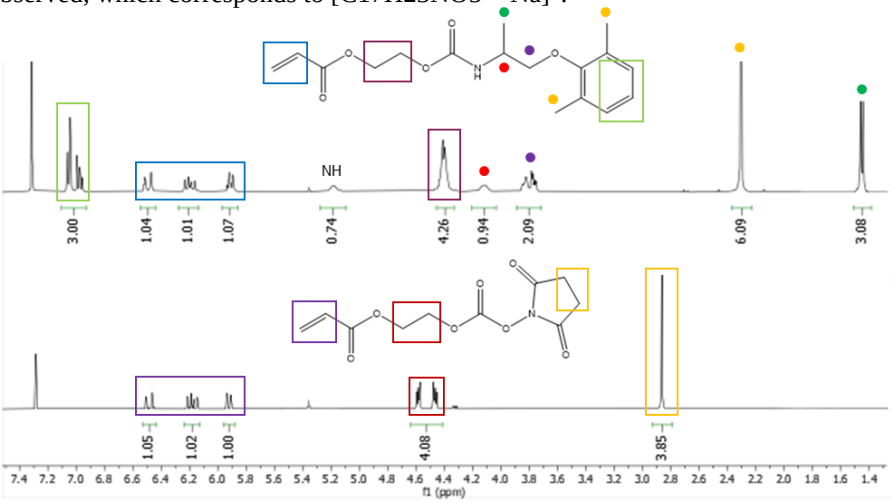

Fig. 7. ^{1}H-NMR spectrum of a)2-((((2,5-dioxopyrrolidin-1-yl)oxy)carbonyl)oxy)ethyl acrylate; b) mexiletine carbamate prodrug.

3.4 Ink Preparation and Casting

To test the potential of the three synthesised prodrugs for use in additive manufacturing, they were formulated as inks for casting. If the inks can be cured under UV light, they may also be printed using SLA, DLP and other techniques. Since the amide and carbamate prodrugs of mexiletine are solids, equal masses of N-acryloyl morpholine (ACMO) were added to obtain liquid inks. ACMO is an excellent solvent and diluent [25]. Moreover, Poly(N-acryloyl morpholine), which is hydrophilic and biocompatible, has been used in the development of pharmaceutical science and demonstrated the ability to modulate drug release [26][27]. In the present study, both prodrugs of mexiletine were dissolved in an equal mass of ACMO. Finally, 1% wt of 2,2-Dimethoxy-2-phenylacetophenone was mixed with the monomers as a low-toxicity photoinitiator.

All three ink formulations were cured rapidly under UV light and were fully moulded after 30 seconds. FTIR characterisation of the inks and castings was carried out to assess the conversion of the monomers in the ink formulations.

Fig. 8 shows that two peaks located in the range of 1612-1624 cm^{-1} and 790-808 cm^{-1} disappeared from the spectra of the three ink formulations after curing under UV light. These two peaks represent the C=C stretch and =C–H bend of the acryloyl group. Therefore, it can be assumed that most of the monomers have undergone polymerisation.

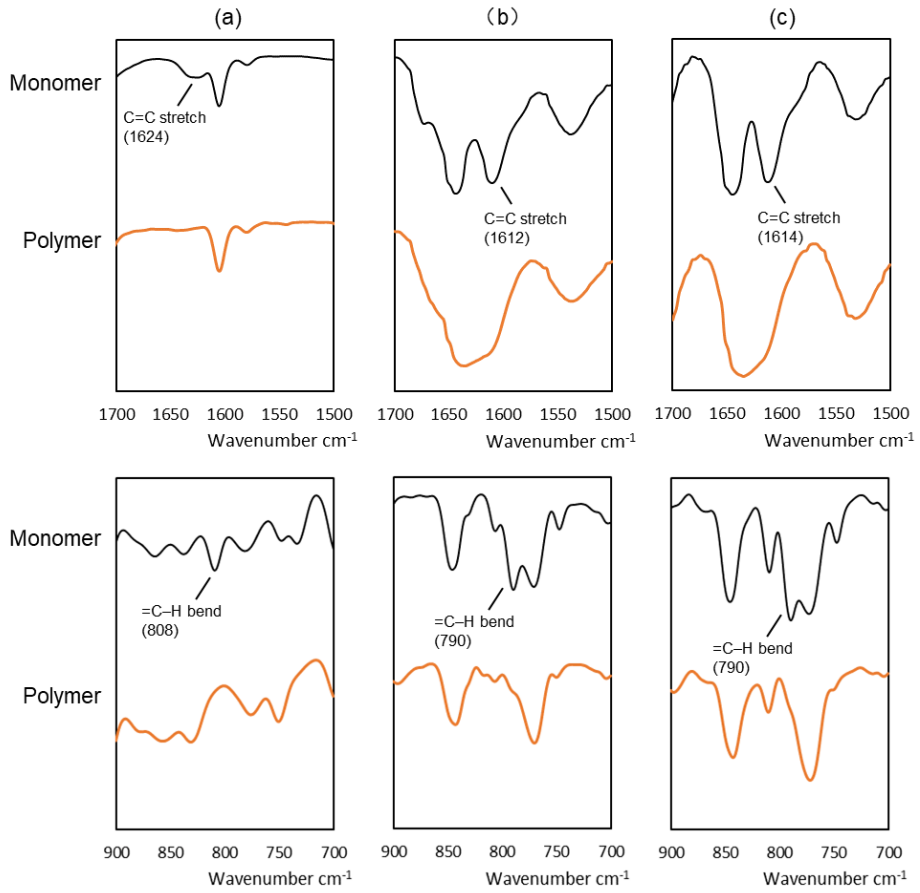

Fig. 8. FTIR spectrum of monomers and polymers with a) aspirin anhydride prodrug; b) mexiletine amide prodrug with ACMO; c) mexiletine carbamate prodrug with ACMO.

3.5 Microscopic Analysis

When designing drug delivery systems using the polymerisation of reactive prodrugs, it is crucial to maintain their chemical stability before administration. If the covalent bond between the drug and the polyacrylate is broken, the drug will be present in the dosage form in a free form. Drugs with hydrogen bond acceptors and donors such as aspirin and mexiletine will aggregate and crystallise through the hydrogen bond. The formation of drug crystals can lead to significant changes in the release profile of the delivery system, which is undesirable. To assess the presence of crystallised drug molecules, casting samples were observed using a microscope with a polarisation analyser (Fig. 9). This method has been widely used to identify the presence of drug crystals, its determined by looking at the lightfield in the darkfield. No visible crystallisation of drug was observed in the samples after casting with three days of storage under dry conditions at room temperature. As a control, 5% mexiletine was dissolved in ACMO and cast. After three days, noticeable drug crystals were observed, although their drug concentrations were much lower than those of the casts containing the original drug (77%, 38%, 28%).

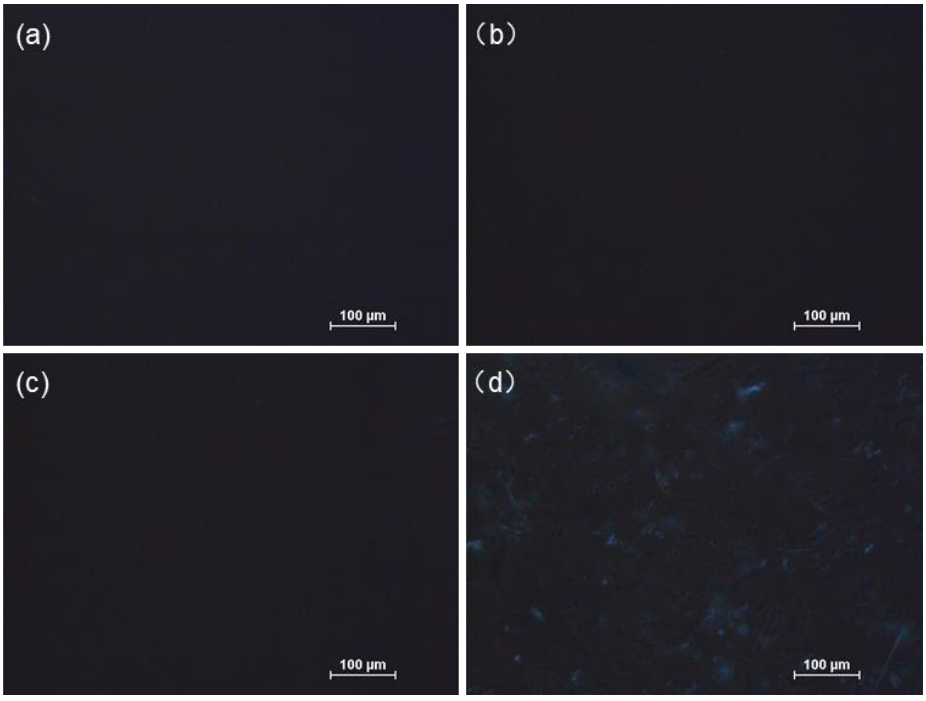

Fig. 9. Polarisation microscopic of casting samples with a) aspirin anhydride prodrug; b) mexiletine amide prodrug with ACMO; c) mexiletine carbamate prodrug with ACMO; d) 5% mexiletine with 95% ACMO.

3.6 Dynamic Mechanical Analysis

The mechanical properties of the casting samples were characterised by dynamic mechanical analysis (Table 1). Since the castings of both the amide and carbamate prodrugs of mexiletine contained ACMO, a sample cured from ACMO and photoinitiator was added as a control. Due to the rigidity of the chains, poly(ACMO) has a high energy storage modulus [29].

The addition of mexiletine amide and carbamate prodrugs resulted in a significant decrease in the storage modulus and higher viscosity of the material. This is because the prodrugs make the polymer side chains softer and the longer side chains increase the intermolecular distances and reduce the interaction forces. This also explains the more significant effect of mexiletine carbamate prodrugs in reducing the storage modulus of the material as compared to the ester prodrugs. The samples made from mexiletine anhydride prodrugs is more viscous than the other two samples due to the absence of ACMO, and they can also be made with different monomers to meet different mechanical property requirements.

Table 1. DMA results of casting samples.

Formulation	Storage modulus (MPa)	Loss modulus (MPa)	tan δ
Aspirin anhydride prodrug	16.7±2.6	13.6±2.2	0.82±0.02
50% Mexiletine amide prodrug + 50% ACMO	252.6±29.4	131.5±2.0	0.53±0.07
50% Mexiletine carbamate prodrug + 50% ACMO	206.4±19.1	133.2±1.0	0.64±0.04
ACMO	783±62.8	80.4±8.2	0.1±0.02

3.7 Dissolution Test

Calibration curves were plotted for aspirin in PBS at pH 2 and pH 7.4 before the dissolution test of the casting samples (Fig. 10). The reason for plotting these two calibration curves separately is that the carboxyl group of aspirin dissociates more readily at pH 7.4, leading to changes in UV absorption [30]. The calibration curve equations obtained with R^2 values greater than 0.999 and the slopes were not significantly different from the calibration curve equations in other studies [31][32].

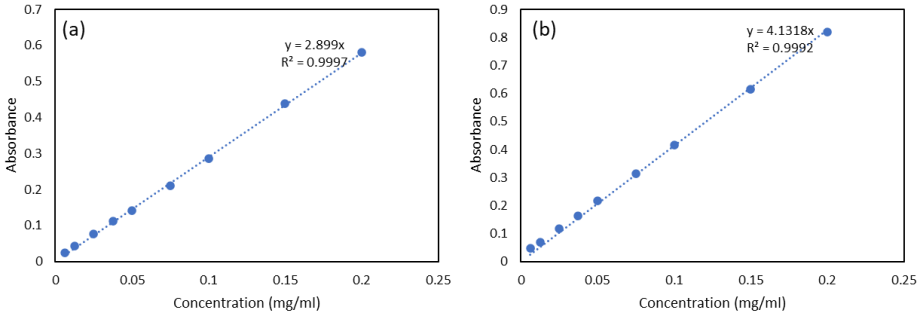

Fig. 10. Calibration curve of aspirin in a) pH 2 PBS buffer; b) pH 7.4 PBS buffer.

Fig. 11 shows the results of the dissolution test. Castings containing the original aspirin anhydride showed a faster release under pH neutral conditions than acidic conditions, since the anhydride bond is less susceptible to hydrolysis under acidic conditions. The castings were all completely dissolved at the end of the dissolution test.

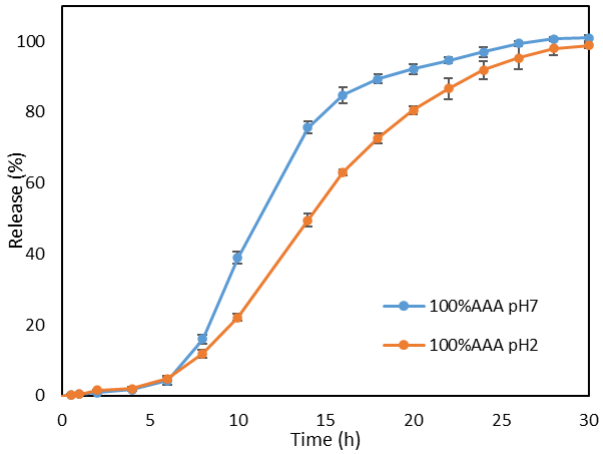

Fig. 11. Release profiles of the casting samples in a) pH 2 PBS buffer; b) pH 7.4 PBS buffer.

3.8 DLP 3D Printing

The ink that includes the prodrug has been proven to solidify when exposed to UV light. With the inclusion of the prodrug aspirin anhydride, the ink formula was successfully printed using a DLP printer (Fig. 12). The printed object was a cylindrical stent-like structure with a 1cm diameter, 1mm wall thickness, and a 1mm square void width. The print displayed high accuracy, indicating that the ink can be used to print complex structures.

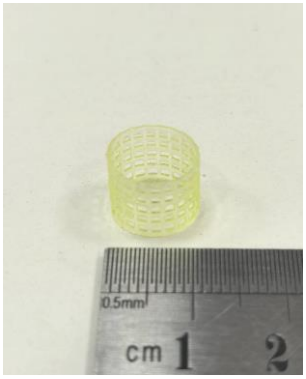

Fig. 12. Sample printed from aspirin anhydride prodrug.

4 Conclusions

In this study, three reactive prodrugs were successfully synthesised with different drugs and breakable covalent bonds. All these prodrug molecules have good light curing properties and can hardly produce drug crystals which could change the drug release profile after polymerisation. These prodrugs have different mechanical properties after curing to meet the requirements of various drug delivery systems. Among them, casts of aspirin anhydride prodrugs were tested for dissolution, demonstrating that aspirin has different release profiles in different pH environments. In addition, printing of ink made from this prodrug was attempted and successful. These provide more available materials for the application of additive manufacturing technology in pharmaceutical sciences and more possibilities for the design of controlled release drug delivery systems.

5 Acknowledgement

This work was supported by the Engineering and Physical Sciences Research Council Award ‘Dialing up Performance for on Demand Manufacturing’ [EP/W017032/1]

References

1. MacDonald, E., & Wicker, R. (2016). Multiprocess 3D printing for increasing component functionality. Science, 353(6307), aaf2093.
2. Conner, B. P., Manogharan, G. P., Martof, A. N., Rodomsky, L. M., Rodomsky, C. M., Jordan, D. C., & Limperos, J. W. (2014). Making sense of 3-D printing: Creating a map of additive manufacturing products and services. Additive manufacturing, 1, 64-76.
3. Praveena, B. A., Lokesh, N., Buradi, A., Santhosh, N., Praveena, B. L., & Vignesh, R. (2022). A comprehensive review of emerging additive manufacturing (3D printing technology): Methods, materials, applications, challenges, trends and future potential. Materials Today: Proceedings, 52, 1309-1313.
4. Kotta, S., Nair, A., & Alsabeelah, N. (2018). 3D printing technology in drug delivery: recent progress and application. Current pharmaceutical design, 24(42), 5039-5048.
5. Jain, V., Haider, N., & Jain, K. (2018). 3D printing in personalized drug delivery. Current pharmaceutical design, 24(42), 5062-5071.
6. Vaz, V. M., & Kumar, L. (2021). 3D printing as a promising tool in personalized medicine. Aaps Pharmscitech, 22, 1-20.
7. Prasad, L. K., & Smyth, H. (2016). 3D Printing technologies for drug delivery: a review. Drug development and industrial pharmacy, 42(7), 1019-1031.
8. Goole, J., & Amighi, K. (2016). 3D printing in pharmaceutics: A new tool for designing customized drug delivery systems. International journal of pharmaceutics, 499(1-2), 376-394.

9. Mohammed, A. A., Algahtani, M. S., Ahmad, M. Z., Ahmad, J., & Kotta, S. (2021). 3D Printing in medicine: Technology overview and drug delivery applications. Annals of 3D Printed Medicine, 4, 100037.
10. Trenfield, S. J., Madla, C. M., Basit, A. W., & Gaisford, S. (2018). Binder jet printing in pharmaceutical manufacturing. 3D printing of pharmaceuticals, 41-54.
11. Sen, K., Manchanda, A., Mehta, T., Ma, A. W., & Chaudhuri, B. (2020). Formulation design for inkjet-based 3D printed tablets. International journal of pharmaceutics, 584, 119430.
12. Patel, S. K., Khoder, M., Peak, M., & Alhnan, M. A. (2021). Controlling drug release with additive manufacturing-based solutions. Advanced drug delivery reviews, 174, 369-386.
13. Mahmood, M. A. (2021). 3D printing in drug delivery and biomedical applications: a state-of-the-art review. Compounds, 1(3), 94-115.
14. Geraili, A., Xing, M., & Mequanint, K. (2021). Design and fabrication of drug-delivery systems toward adjustable release profiles for personalized treatment. View, 2(5), 20200126.
15. Khaled, S. A., Burley, J. C., Alexander, M. R., & Roberts, C. J. (2014). Desktop 3D printing of controlled release pharmaceutical bilayer tablets. International journal of pharmaceutics, 461(1-2), 105-111.
16. Zhang, J., Feng, X., Patil, H., Tiwari, R. V., & Repka, M. A. (2017). Coupling 3D printing with hot-melt extrusion to produce controlled-release tablets. International journal of pharmaceutics, 519(1-2), 186-197.
17. Zhang, J., Yang, W., Vo, A. Q., Feng, X., Ye, X., Kim, D. W., & Repka, M. A. (2017). Hydroxypropyl methylcellulose-based controlled release dosage by melt extrusion and 3D printing: Structure and drug release correlation. Carbohydrate polymers, 177, 49-57.
18. He, Y., Foralosso, R., Trindade, G. F., Ilchev, A., Ruiz-Cantu, L., Clark, E. A., ... & Wildman, R. D. (2020). A reactive prodrug ink formulation strategy for inkjet 3D printing of controlled release dosage forms and implants. Advanced Therapeutics, 3(6), 1900187.
19. Li, Y., Bai, Y., Pan, J., Wang, H., Li, H., Xu, X., ... & Wei, S. (2019). A hybrid 3D-printed aspirin-laden liposome composite scaffold for bone tissue engineering. Journal of materials chemistry B, 7(4), 619-629.
20. Frommeyer, G., Garthmann, J., Ellermann, C., Dechering, D. G., Kochhäuser, S., Reinke, F., ... & Eckardt, L. (2018). Broad antiarrhythmic effect of mexiletine in different arrhythmia models. EP Europace, 20(8), 1375-1381.
21. Maines, E. M., Porwal, M. K., Ellison, C. J., & Reineke, T. M. (2021). Sustainable advances in SLA/DLP 3D printing materials and processes. Green Chemistry, 23(18), 6863-6897.
22. Shahzadi, L., Maya, F., Breadmore, M. C., & Thickett, S. C. (2022). Functional materials for DLP-SLA 3D printing using thiol–acrylate chemistry: Resin design and postprint applications. ACS Applied Polymer Materials, 4(5), 3896-3907.
23. Cai, L., & Wang, S. (2010). Elucidating colorization in the functionalization of hydroxyl-containing polymers using unsaturated anhydrides/acyl chlorides in the presence of triethylamine. Biomacromolecules, 11(1), 304-307.
24. Tarducci, C., Schofield, W. C. E., Badyal, J. P. S., Brewer, S. A., & Willis, C. (2002). Synthesis of cross-linked ethylene glycol dimethacrylate and cyclic methacrylic anhydride polymer structures by pulsed plasma deposition. Macromolecules, 35(23), 8724-8727.
25. Grigale-Soročina, Z., Vindedze, E., Kozela, J., & Birks, I. (2021). Evaluation of Reactive Diluent Impact on Stability of Systems Viscosity in UV-Curable Compositions. Solid State Phenomena, 320, 150-154.

26. Arsenie, L. V., Ladmiral, V., Desmazes, P. L., & Catrouillet, S. (2023). Morpholine and thiomorpholine derived polymers: Multifunctional platforms for biological applications. European Polymer Journal, 112490.
27. Abou Taleb, M. F., El-Sigeny, S., & El-Kemary, M. (2012). Sustained-release of flutamide from radiation-crosslinked poly (4-acryloyl morpholine-acrylic acid) hydrogels. Macromolecular Research, 20, 407-414.
28. Yu, D. G., Shen, X. X., Zhang, X. F., Zhu, L. M., Branford-White, C., & White, K. (2009, August). Applications of polarization microscope in determining the physical status of API in the wet-spinning drug-loaded fibers. In 2009 Symposium on Photonics and Optoelectronics (pp. 1-4). IEEE.
29. Huang, W., Zhang, J., Singh, V., Xu, L., Kabi, P., Bele, E., & Tiwari, M. K. (2023). Digital light 3D printing of a polymer composite featuring robustness, self-healing, recyclability and tailorable mechanical properties. Additive Manufacturing, 61, 103343.
30. Sharma, V., Bhowmick, M., Rathi, V., & Rathi, J. (2017). Preformulation, precompression and post compression evaluation of bilayer tablet of aspirin as immediate release and nicotinic acid as sustained release. Int J Pharm Chem Biol Sci, 7, 55-70.
31. Wang, Y., Xu, P. P., Li, X. X., Nie, K., Tuo, M. F., Kong, B., & Chen, J. (2012). Monitoring the hydrolyzation of aspirin during the dissolution testing for aspirin delayed-release tablets with a fiber-optic dissolution system. Journal of pharmaceutical analysis, 2(5), 386-389.
32. Yamauchi, Y., Doi, N., Kondo, S. I., Sasai, Y., & Kuzuya, M. (2020). Characterization of a novel polymeric prodrug of an antibacterial agent synthesized by mechanochemical solid‐state polymerization. Drug Development Research, 81(7), 867-874.